applied sciences

MDPI

Article

Chemical Investigation of Diketopiperazines and N-Phenethylacetamide Isolated from *Aquimarina* sp. MC085 and Their Effect on TGF-β-Induced Epithelial–Mesenchymal Transition

Myong Jin Lee [1,†], Geum Jin Kim [2,3,†], Myoung-Sook Shin [1], Jimin Moon [2], Sungjin Kim [1], Joo-Won Nam [2], Ki Sung Kang [1,*] and Hyukjae Choi [2,3,*]

[1] College of Korean Medicine, Gachon University, Seongnam 13120, Korea; myongene@naver.com (M.J.L.); ms.shin@gachon.ac.kr (M.-S.S.); qkrnsld@naver.com (S.K.)
[2] College of Pharmacy, Yeungnam University, Gyeongsan 38541, Korea; kimgeumjin@naver.com (G.J.K.); hyp1112@yu.ac.kr (J.M.); jwnam@yu.ac.kr (J.-W.N.)
[3] Research Institute of Cell Culture, Yeungnam University, Gyeongsan 38541, Korea
* Correspondence: kkang@gachon.ac.kr (K.S.K.); h5choi@yu.ac.kr (H.C.); Tel.: +82-31-750-5402 (K.S.K.); +82-53-810-2824 (H.C.)
† These authors contributed equally to this work.

Abstract: Chemical investigations of *Aquimarina* sp. MC085, which suppressed TGF-β-induced epithelial–mesenchymal transition (EMT) in A549 human lung cancer cells, led to the isolation of compounds **1**–**3**. Structural characterization using spectroscopic data analyses in combination with Marfey's analysis revealed that they were two diketopiperazines [*cyclo*(L-Pro-L-Leu) (**1**) and *cyclo*(L-Pro-L-Ile) (**2**)] and one N-phenethylacetamide (**3**). *Cyclo*(L-Pro-L-Leu) (**1**) and N-phenethylactamide (**3**) inhibited the TGF-β/Smad pathway and suppressed the metastasis of A549 cells by affecting TGF-β-induced EMT. However, *cyclo*(L-Pro-L-Ile) (**2**) downregulated mesenchymal factors via a non-Smad-mediated signaling pathway.

Keywords: *Aquimarina* sp.; diketopiperazine; N-phenethylacetamide; epithelial-mesenchymal transition (EMT); A549 cells

Citation: Lee, M.J.; Kim, G.J.; Shin, M.-S.; Moon, J.; Kim, S.; Nam, J.-W.; Kang, K.S.; Choi, H. Chemical Investigation of Diketopiperazines and N-Phenethylacetamide Isolated from *Aquimarina* sp. MC085 and Their Effect on TGF-β-Induced Epithelial–Mesenchymal Transition. *Appl. Sci.* **2021**, *11*, 8866. https://doi.org/10.3390/app11198866

Academic Editor: Panagiota Diamantopoulou

Received: 6 August 2021
Accepted: 18 September 2021
Published: 23 September 2021

1. Introduction

Marine natural products are considered as rich sources of cytotoxins, many of which could serve as lead compounds for anticancer drug development [1]. Recently, many marine natural products have become accepted as the biosynthetic products of marine microorganisms [2]. Chemical investigations on marine microorganisms have resulted in the discovery of anticancer agents, such as bretuximab vedotin and salinosporamide A [3].

Epithelial–mesenchymal transition (EMT) is an important morphological process that differentiates epithelial cells into mesenchymal phenotype. It is characterized by the loss of polarity, cell–cell contact, and gain of mesenchymal markers. Epithelial cadherin is degraded in the plasma membrane, and desmosomes are inhibited by transcription. EMT facilitates the migration and invasion of cancer cells [4–6]. Therefore, EMT inhibitors are effective in cancer chemotherapy, particularly against metastasis.

For many years, plant-derived natural products such as arctigenin [4], betanin [5], camosol [6], curcumin [7], paeoniflorin [8], and tannic acid [9] have been known to regulate EMT-related signaling pathways. However, a few marine derived natural products were also reported to have EMT-modulating activities. Eribulin mesylate, a marine-derived natural product and FDA-approved anticancer drug, is an EMT inhibitor [10]. In addition, marine microbial natural products such as biemamides [11], actinomycin V [12], pentabromopseudilin [13], and androsamide [14] were shown to target the EMT signaling pathway.

As part of our efforts to discover bioactive natural products from marine microorganisms, we found that the ethyl acetate extract of marine-derived *Aquimarina* sp. MC085 inhibited TGF-β-induced EMT in A549 cells. The genus *Aquimarina* belongs to the family *Flavobacteriaceae* and is known for its aerobic and halophilic characteristics. Chemical investigations of this genus were rarely reported. The *Aquimarina* genus was reported to produce algicidal proteins against toxic cyanobacterium *Microcystis aeruginosa* [15]. Genome mining of *Aquimarina* sp. Ap349 resulted in the discovery of cuniculenes 6A and 6 B derived from polyketide synthase [16]. However, no other natural product with biological activity was reported from the bacterium in this genus. Bioactivity-guided isolation and chemical investigations of *Aquimarina* sp. MC085 led to the isolation of three natural products, and a spectroscopic data analysis led to the structural assignment of the isolates.

2. Materials and Methods

2.1. General Experimental Procedure

Optical rotation was measured using a Jasco DIP-1000 polarimeter (Tokyo, Japan). Nuclear magnetic resonance (NMR) spectra were recorded using a 250 MHz Bruker NMR spectrometer (DMX 250) and 600 MHz Varian NMR spectrometer (VNS-600, Palo Alto, Santa Clara, CA, USA) at the Core Research Support Center for Natural Products and Medical Materials (CRCNM). Low-resolution electrospray ionization MS (LR–ESI–MS) was performed using an Agilent 6120 single-quadrupole mass spectrometer (Agilent Technologies, Santa Clara, CA, USA) with a C3 column (Agilent SB-C3 Zorbax, 5 μm, 4.6 × 150 mm). Isolation of the compounds was carried out using a Waters 1525 binary high-performance liquid chromatography (HPLC) pump having a Waters 996 photodiode array (PDA) with a reversed-phase HPLC (RS Tech, Cheongju, Republic of Korea, Hector-M 5 μm C18, 250 × 4.6 mm).

2.2. Fermentation of Aquimarina sp. MC085 and Preparation of Extracts

The bacterial strain *Aquimarina* sp. MC085 (GenBank Accession No. MG016025) was incubated at 25 °C in a shaking incubator at 150 rpm in 5 L of SYP media. After 7 days, the broth media of strain MC085 was extracted twice with ethyl acetate and the combined extract was evaporated.

2.3. Acid Hydrolysis and C3 Marfey's Analysis of Compounds ***1*** and ***2***

Each compound (100 μg) was dissolved in 6 N HCl (400 μL) in 4 mL glass vials. The vials were incubated at 110 °C for 4 h with stirring. The resulting acid hydrolysates were dried under a stream of N_2 gas. The dried acid hydrolysates were resuspended in deionized water. After the removal of water under a N_2 gas stream, the hydrolysates were dissolved in 40 μL of MeOH and treated with 60 μL of 1.0 M $NaHCO_3$ and 25 μL of 1% L-FDAA (1-fluoro-2,4-dinitrophenyl-5-L-alanine amide) in acetone. The reaction mixtures in each vial were incubated at 40 °C for 1 h with stirring, and the reaction was quenched by the addition of 60 μL of 1 N HCl. The resulting solutions (10 μL) were injected to LC-ESI-MS; Agilent Zorbax SB-C3 column, 5 μm, 150 × 4.6 mm, 50 °C, 1.0 mL/min, solvent A (deionized water), solvent B [95% MeOH + 5% of (95% CH3CN + 5% formic acid)], A:B = 70:30→45:55 (95 min)→0:100 (97 min)→0:100 (104 min)→70:30 (105 min)→70:30 (110 min). The reaction products with FDAA-derivatized hydrolysates were analyzed in the negative mode of the LC-MS system. The retention time of the DAA-derivatives of constituting amino acids was compared with that of the authentic standards (DAA-L-Pro: 15.5 min, DAA-D-Pro: 19.0 min, DAA-L-*allo*-Ile: 39.5 min, DAA-L-Ile: 41.8 min, DAA-L-Leu: 42.6 min, DAA-D-*allo*-Ile: 61.7 min, DAA-D-Ile: 64.5 min, DAA-D-Leu: 65.0 min).

2.4. Cell Culture and Treatment

A549 (human lung carcinoma epithelial) cells were incubated in RPMI 1640 medium supplemented with 10% (*v*/*v*) fetal bovine serum and 1% penicillin–streptomycin at 37 °C in a humidified atmosphere of 5% CO_2 and 95% air. The cells were then treated with

compounds **1**–**3**, respectively, in medium for 6 h. This was followed by treatment with TGF-β (5 ng/mL) for 42 h in the presence or absence of compounds at the indicated concentrations.

2.5. Cell Viability Assay

An EZ-Cytox assay kit (DoGenBio, Seoul, Korea) was used to assess cell viability. Cells (5×10^4 cells/well) were seeded into a 96-well plate. After 24 h, compounds **1**–**3** were added to serum-free medium for 6 h before TGF-β (5 ng/mL) stimulation. EZ-Cytox reagent was added to the plate and incubated for 1 h at 37 °C. The absorbance at 450 nm was measured using an enzyme-linked immunosorbent assay (ELISA) plate reader.

2.6. Western Blotting Analysis

A549 cells were treated with compounds **1**–**3**, as previously described. After 6 h, cells were treated with 5 ng/mL of TGF-β with or without each peptide for 42 h. Cells were lysed in RIPA buffer (50 mM Tris-HCl pH 7.4, 150 mM NaCl, 0.25% deoxycholate, 1% NP-40, and 1 mM EDTA), and protein concentration was determined using BCA reagent (ThermoScientific, Rockford, IL, USA) according to the manufacturer's instructions.

Proteins were separated by sodium dodecyl sulfate polyacrylamide gel electrophoresis (SDS-PAGE) and then transferred to polyvinylidene difluoride (PVDF) membranes (Millipore, Burlington, MA, USA). After the transfer, membranes were blocked with 5% nonfat dried milk/TBST (20 mM Tris pH 7.4, 150 mM NaCl, and 0.2% Tween-20) for 1 h and then incubated overnight at 4 °C with primary antibody. The antibodies used were anti-Smad2/3, phosphorylated Smad2/3, N-cadherin, E-cadherin, Vimentin, Snail, β-catenin, and GAPDH from Cell Signaling Technology (Danvers, MA, USA). After the wash with TBST, the membranes were probed with HRP-labeled secondary antibodies. Finally, an enhanced chemiluminescence detection kit (Fisher Scientific, Rockford, IL, USA) was used to visualize the immunoreactive proteins.

2.7. Gelatin Zymography

Cell supernatants of serum-free cultures were concentrated using Amicon Ultra-4 Centrifugal Filter Devices (Millipore, Billerica, MA, USA). Matrix Metalloproteinase-2 (MMP-2) activity was determined using a Zymogram–PAGE System (Komabiotech, Seoul, Korea) according to the manufacturer's instructions. In brief, after electrophoresis, the gel was washed for 30 min to remove the SDS and then incubated overnight at 37 °C with a developing buffer. Then, the gel was stained with Coomassie Blue R-250 and distained with methanol and acetic acid. The gelatinolytic activities were then visualized as a white band and the gels were scanned.

2.8. Statistical Analysis

Results are expressed as mean ± standard deviations (SD). The statistical significance between test groups was determined using a one-way ANOVA multiple comparison test with Turkey's post-test using GraPhad Prism 5 software (GraphPad Software Inc., San Diego, CA, USA). $p < 0.05$ was considered statistically significant.

3. Results

3.1. Structural Identification of Compounds *1*–*3*

Compound **1** was obtained as a white powder, {$[\alpha]^{22}_D$ −54.47° (*c* 0.14, CH_3OH)}. The ^{13}C NMR spectrum of **1** in DMSO-*d6* showed distinctive 11 carbon signals including two amide carbonyls at δ_C 170.32 and 166.51, three sp3 carbons with the attachment of N atom at δ_C 58.44, 52.59, and 44.83, and six sp3 carbons without N attachment at δ_C 37.76, 27.40, 24.04, 22.79, 22.44, and 21.88. The ^1H NMR spectrum of **1** in DMSO-*d6* showed a broad NH proton signal at δ_H 8.00, signals for two α protons at δ_H 4.19, and 4.00, N-attached methylene protons at δ_H 3.42–3.30, two doublet methyl signals at δ_H 0.87 (*J* = 6.3 Hz) and 0.86 (*J* = 6.3 Hz), along with the residual seven protons at δ_H 2.22–1.30. The ESI-MS

spectrum (positive ion detection mode) showed a peak corresponding to a protonated molecule at m/z 211.4 $[M + H]^+$. These data indicated that the molecular formula of compound **1** was $C_{11}H_{18}N_2O_2$. The 2D NMR data analysis led to the planar structure of **1** as a cyclic dipeptide, *cyclo*(Pro-Leu), as shown in Figure 1. The absolute configuration of **1** was determined to be *cyclo*(L-Pro-L-Leu) using C3 Marfey's method (Figure S8) [17].

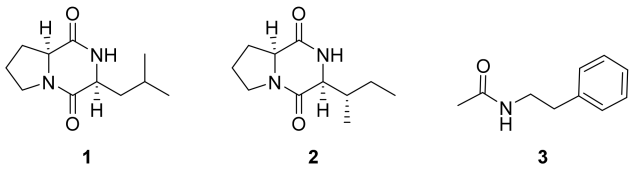

Figure 1. Structures of compounds **1**–**3** from *Aquimarina* sp. MC085.

Compound **2** $\{[\alpha]^{22}_D$ −48.65° (*c* 0.07, $CH_3OH)\}$ showed a protonated ion at m/z 211.4 $[M + H]^+$ in the positive ion mode of the ESI-MS spectrum. The ^1H NMR spectrum of **2** showed structural features similar to those of compound **1**. However, compound **2** showed a distinctive methyl triplet and a methyl doublet, whereas compound **1** showed two methyl doublets. Based on a careful comparison of spectroscopic data, including ^1H and ^{13}C NMR data, compound **2** was identified as *cyclo*(Pro-Ile). In addition, C3 Marfey's analyses configured both constituting amino acids as L (Figure S9) [17].

Compound **3** was obtained as a white powder. Its molecular formula was assigned as $C_{10}H_{13}NO$ based on 1D NMR spectra and the presence of a protonated ion at m/z 164.2 $[M + H]^+$ in the ESI-MS spectrum. The ^1H and ^{13}C NMR spectra of compound **3** in $CDCl_3$ showed five proton signals in the ranges of δ_H 7.15–7.35, and resonances for four sp2 methine carbons at δ_C 138.97, 128.80, 128.69, and 126.57, corresponding to a mono-substituted phenyl ring. Moreover, signals of two methylene units (δ_C 40.78, δ_H 2.80; δ_C 35.68, δ_H 3.49) and an acetyl unit (δ_C 170.35; δ_C 23.30, δ_H 1.92) were observed. By comparing the spectroscopic data with the values provided in the literature, the structure of compound **3** was confirmed to be N-phenethylacetamide [18]. Compounds **1**–**3** were isolated from microorganisms of the genus *Aquimarina* for the first time.

*3.2. The Cell Viability Effect on Comparison of Compounds **1**–**3** on TGF-β-Induced EMT of A549 Cells*

First, we investigated the cytotoxic effects of compounds **1**–**3** with or without TGF-β on A549 cells using an EZ-Cytox assay. As presented in Figure 2, the cells were treated with various concentrations of compounds **1**–**3** (100, 50, 25, and 12.5 μM) for 24 h. The cell viability analysis showed that none of the components affected cell viability at concentrations below 50 μM; however, compound **2** showed a significant decrease cell viability at 100 μM concentration. Therefore, further assays were conducted at a concentration of 50 μM.

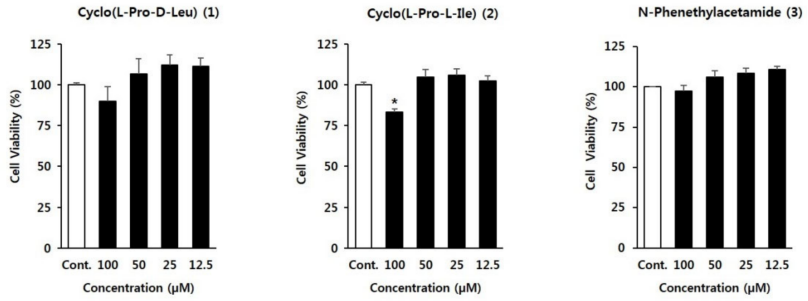

Figure 2. Comparison of the effects of compounds **1**–**3** on TGF-β-induced epithelial to mesenchymal transition (EMT) of A549 cells. The cells were treated with different concentrations of **1**–**3** before TGF-β treatment for 24 h and viability was determined using the EZ-Cytox assay. The data represent the means ± S.D. of three independent experiments. * $p < 0.05$ compared with the control.

*3.3. Comparison of the Protein Expression Profiles of A549 Cells to Determine the Effect of the Treatment with Compounds **1**–**3** (50 μM), via the Smad2/3 Signaling Pathway, on the TGF-β-Mediated EMT of the Cells*

To observe the expression levels of proteins associated with canonical Smad2/3, A549 cells were treated with 50 μM of the test compounds, followed by a TGF-β treatment. Phosphorylation of Smad2/3 was measured using western blotting. On comparison with the control group, the results showed that TGF-β induced the phosphorylation of Smad2/3. Phosphorylated Smad2/3 was inhibited by compounds **1** and **3** (Figure 3A). We also examined the effect of compounds **1**–**3** on TGF-β-mediated expression of EMT-related markers in A549 cells. N-Phenethylacetamide (**3**) dramatically downregulated mesenchymal phenotypic markers (N-cadherin, vimentin, and Snail) induced by TGF-β (p = 0.0014). The levels of vimentin and Snail were reduced by compound **2** in the TGF-β-treated A549 cells. However, β-catenin levels were not changed in the compounds **1**–**3**-treated cells exposed or not exposed to TGF-β (Figure 3B).

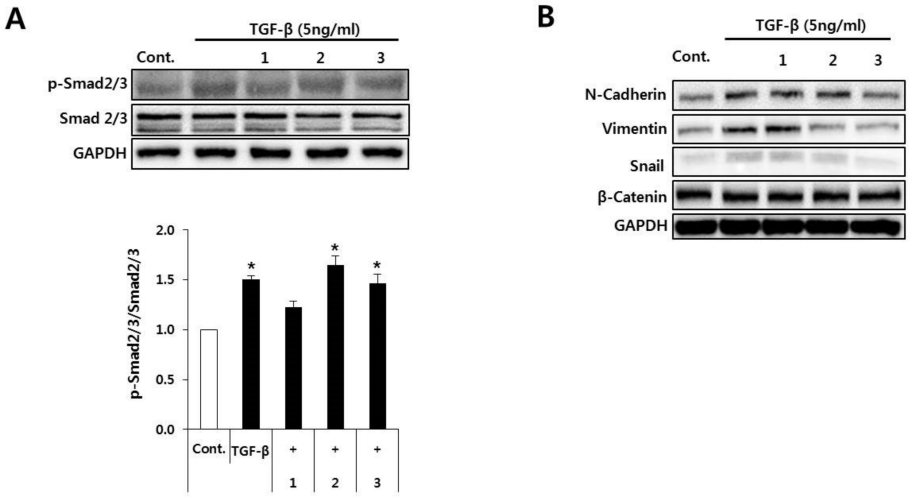

Figure 3. Comparison of the protein expression profiles of A549 cells to determine the effect of the treatment with compounds **1**–**3** (50 μM, respectively), via the Smad2/3 signaling pathway, on the TGF-β-mediated EMT of the cells. (**A**) Phosphorylation of Smad2/3 was detected by Western blot analysis and densitometry. Error bars denote SD from three independent replicates. (*) indicates statistical significance ($p < 0.05$) when compared to control. (**B**) The levels of TGF-β-induced EMT-related markers were determined by Western blotting.

*3.4. Comparison of the Effects of the Compounds **1**–**3** (50 μM) on the Activity of MMP-2 in A549 Human Lung Carcinoma Cells, Tested Using Gelatin Zymography*

MMP-2 is the main proteolytic collagenase among MMPs and plays a major role in the invasion and metastasis of cancer cells. Therefore, we investigated the effects of compounds **1**–**3** on MMP-2 activity. The 62-KDa form was identified as MMP-2. MMP-2 expression was increased by TGF-β stimulation. All cells treated with compounds **1**–**3** showed decreased MMP-2 activity compared to cells subjected to TGF-β treatment alone (Figure 4).

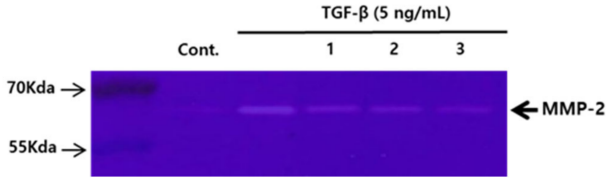

Figure 4. Comparison of the effects of compounds **1**–**3** (50 μM) on matrix metalloproteinase-2 (MMP-2) activity in A549 human lung carcinoma cells, tested using gelatin zymography. The cell supernatants were harvested and concentrated by centrifugation using Amicon Ultra-4 centrifugal filter devices. Clear bands represent gelatin-cleaved areas.

4. Discussion

EMT is induced by several signaling pathways, including transforming growth factor-β1 (TGF-β1), hypoxia, notch, and hedgehog [19]. In our study, EMT of human lung cancer A549 cells was induced by TGF- β. EMT is characterized by the loss of epithelial markers, including vimentin, N-cadherin, fibronectin, and α-smooth muscle actin, and an increase in mesenchymal markers [20]. Therefore, we analyzed the protein expression of mesenchymal markers by immunoblotting. MMP-2 is a proteolytic enzyme that induces EMT by breaking down the extracellular matrix of malignant cells [21]. In this study, MMP-2 activity was evaluated using gelatin zymography.

Compound **1** is known to have diverse bioactivities, including antibacterial [22], antifungal [23], antifouling [24], anti-biofilm activities [25], quorum sensing modulation [26,27], inhibition of dengue virus replication [28], and induction of mitochondria-mediated apoptosis and tumor growth suppression [29]. Compound **2** was reported to have antifungal [30] and quorum sensing inhibitory activities [26]. Compound **3** was reported to inhibit chymotrypsin A [31], increase the lifespan of *Caenorhabditis elegans* by SIR-2.1 induction [32], and reverse the resistance of doxorubicin-resistant leukemia P388 cells [33]. However, the EMT-related bioactivities of compounds **1**–**3** were not previously investigated. Compounds **1** and **3** downregulated MMP-2 through the inhibition of TGF-β-mediated phosphorylation of Smad2/3 in A549 cells. Compound **3** also reversed TGF-β-induced EMT markers, N-cadherin, vimentin, and Snail. Although compound **2** exhibited activities through a non-Smad-mediated signaling pathway, it attenuated TGF-β-dependent induction of mesenchymal markers, such as vimentin and Snail. In addition, it modulated the expression level of MMP-2 compared to that in the untreated controls in the A549 cell line. High MMP expression is associated with tumor invasion and metastasis. The present study showed that the increased expression of MMP-2 by TGF-β treatment was inhibited by compounds **1**–**3** (Figure 5). Smad2/3 activated by TGF-β induction translocates to the nucleus, and β-catenin might form a complex with active Smad2/3. The complex may interact with various transcription factors and regulate EMT-related genes. *Cyclo*(L-Pro-L-Leu) (**1**) and N-phenethylactamide (**3**) inhibited TGF-β/Smad pathways and suppressed metastasis of A549 cells by affecting TGF-β-induced EMT. However, *cyclo*(L-Pro-L-Ile) (**2**) downregulated mesenchymal factors via a non-Smad-mediated signaling pathway. The chemical investigation of *Aquimarina* sp. MC085 led to the identification of two diketopiperazines [*cyclo*(L-Pro-L-Leu) (**1**) and *cyclo*(L-Pro-L-Ile) (**2**)] and one N-phenethylacetamide (**3**), which inhibit TGF-β-mediated EMT.

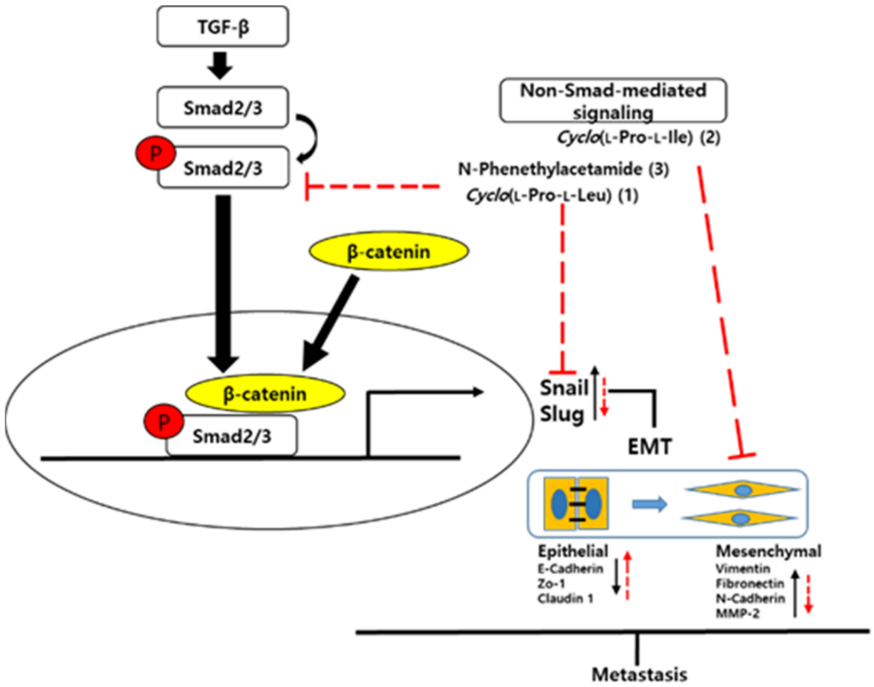

Figure 5. Proposed mechanism of action of compounds **1**–**3** on TGF-β-induced EMT of A549 cells.

5. Conclusions

The chemical investigation of *Aquimarina* sp. MC085 led to the isolation of compounds **1**–**3**, which suppressed TGF-β-induced EMT of A549 human lung cancer cells. *Cyclo*(L-Pro-L-Leu) (**1**) and N-phenethylactamide (**3**) inhibited TGF-β/Smad pathways and suppressed the metastasis of A549 cells by affecting TGF-β-induced EMT. However, *cyclo* (L-Pro-L-Ile) (**2**) downregulated mesenchymal factors via a non-Smad-mediated signaling pathway.

Supplementary Materials: The following are available online at https://www.mdpi.com/article/10.3390/app11198866/s1, Figure S1: LR-ESI-MS data of **1**; Figure S2: ^{1}H NMR spectrum (250 MHz) of **1** in DMSO-d_6; Figure S3: ^{13}C NMR (63 MHz) spectrum of **1** in DMSO-d_6; Figure S4: HMQC spectrum of **1** in DMSO-d_6; Figure S5: HMBC spectrum of **1** in DMSO-d_6; Figure S6: ^{1}H NMR spectrum (600 MHz) of **1** in CD_3OD; Figure S7: ^{13}C NMR (150 MHz) spectrum of **1** in CD_3OD; Figure S8: C3 Marfey's analysis of **1**; Figure S9: LR-ESI-MS data of **2**; Figure S10: ^{1}H NMR spectrum (250 MHz) of **2** in CD_3OD; Figure S11: ^{3}C NMR (63 MHz) spectrum of **2** in CD_3OD; Figure S12: C3 Marfey's analysis of **2**; Figure S13: LR-ESI-MS data of **3**; Figure S14: ^{1}H NMR spectrum (250 MHz) of **3** in $CDCl_3$; Figure S15: ^{13}C NMR (63 MHz) spectrum of **3** in $CDCl_3$.

Author Contributions: Conceptualization, K.S.K. and H.C.; formal analysis, M.J.L., G.J.K., M.-S.S., J.M. and S.K.; investigation, M.J.L. and J.-W.N.; writing—original draft preparation, M.J.L., G.J.K. and H.C.; writing—review and editing, K.S.K.; visualization, M.J.L. and G.J.K.; supervision, K.S.K. and H.C.; project administration, K.S.K. and H.C.; funding acquisition, K.S.K. and H.C. All authors have read and agreed to the published version of the manuscript.

Funding: This research was supported by the 2020 Yeungnam University Research Grants and the research grants from the Basic Science Research Program through the National Research Foundation of Korea (NRF) (grant number: 2019R1F1A1059173 and 2020R1A6A1A03044512).

Institutional Review Board Statement: Not applicable.

Informed Consent Statement: Not applicable.

Data Availability Statement: The data that support the findings of this study are available from the corresponding author upon reasonable request.

Conflicts of Interest: The authors declare no conflict of interest.

References

1. Newman, D.J.; Cragg, G.M. Natural products as sources of new drugs over the nearly four decades from 01/1981 to 09/2019. *J. Nat. Prod.* **2020**, *83*, 770–803. [CrossRef] [PubMed]
2. Gerwick, W.H.; Moore, B.S. Lessons from the past and charting the future of marine natural products drug discovery and chemical biology. *Chem. Biol.* **2012**, *19*, 85–98. [CrossRef] [PubMed]
3. Jiménez, C. Marine Natural Products in Medicinal Chemistry. *ACS Med. Chem. Lett.* **2018**, *9*, 959–961. [CrossRef] [PubMed]
4. Xu, Y.; Lou, Z.; Lee, S.-H. Arctigenin represses TGF-β-induced epithelial mesenchymal transition in human lung cancer cells. *Biochem. Biophys. Res. Commun.* **2017**, *493*, 934–939. [CrossRef]
5. Sutariya, B.; Saraf, M. Betanin, isolated from fruits of Opuntia elatior Mill attenuates renal fibrosis in diabetic rats through regulating oxidative stress and TGF-β pathway. *J. Ethnopharmacol.* **2017**, *198*, 432–443. [CrossRef]
6. Giacomelli, C.; Daniele, S.; Natali, L.; Iofrida, C.; Flamini, G.; Braca, A.; Trincavelli, M.L.; Martini, C. Carnosol controls the human glioblastoma stemness features through the epithelial-mesenchymal transition modulation and the induction of cancer stem cell apoptosis. *Sci. Rep.* **2017**, *7*, 15174. [CrossRef]
7. Li, W.; Jiang, Z.; Xiao, X.; Wang, Z.; Wu, Z.; Ma, Q.; Cao, L. Curcumin inhibits superoxide dismutase-induced epithelial-to-mesenchymal transition via the PI3K/Akt/NF-κB pathway in pancreatic cancer cells. *Int. J. Oncol.* **2018**, *52*, 1593–1602. [CrossRef]
8. Wang, Z.; Liu, Z.; Yu, G.; Nie, X.; Jia, W.; Liu, R.-E.; Xu, R. Paeoniflorin inhibits migration and invasion of human glioblastoma cells via suppression transforming growth factor β-induced epithelial–mesenchymal transition. *Neurochem. Res.* **2018**, *43*, 760–774. [CrossRef]
9. Pattarayan, D.; Sivanantham, A.; Krishnaswami, V.; Loganathan, L.; Palanichamy, R.; Natesan, S.; Muthusamy, K.; Rajasekaran, S. Tannic acid attenuates TGF-β1-induced epithelial-to-mesenchymal transition by effectively intervening TGF-β signaling in lung epithelial cells. *J. Cell. Physiol.* **2018**, *233*, 2513–2525. [CrossRef]
10. Dybdal-Hargreaves, N.F.; Risinger, A.L.; Mooberry, S.L. Eribulin mesylate: Mechanism of action of a unique microtubule-targeting agent. *Clin. Cancer Res.* **2015**, *21*, 2445–2452. [CrossRef]
11. Zhang, F.; Braun, D.R.; Ananiev, G.E.; Hoffmann, F.M.; Tsai, I.-W.; Rajski, S.R.; Bugni, T.S. Biemamides A–E, inhibitors of the TGF-β pathway that block the epithelial to mesenchymal transition. *Org. Lett.* **2018**, *20*, 5529–5532. [CrossRef] [PubMed]
12. Lin, S.; Zhang, C.; Liu, F.; Ma, J.; Jia, F.; Han, Z.; Xie, W.; Li, X. Actinomycin V inhibits migration and invasion via suppressing snail/slug-mediated epithelial-mesenchymal transition progression in human breast cancer MDA-MB-231 cells in vitro. *Mar. Drugs* **2019**, *17*, 305. [CrossRef] [PubMed]
13. Shih-Wei, W.; Chih-Ling, C.; Kao, Y.-C.; Martin, R.; Knölker, H.-J.; Shiao, M.-S.; Chen, C.-L. Pentabromopseudilin: A myosin V inhibitor suppresses TGF-β activity by recruiting the type II TGF-β receptor to lysosomal degradation. *J. Enzym. Inhib. Med. Chem.* **2018**, *33*, 920–935. [CrossRef]
14. Lee, J.; Gamage, C.D.; Kim, G.J.; Hillman, P.F.; Lee, C.; Lee, E.Y.; Choi, H.; Kim, H.; Nam, S.-J.; Fenical, W. Androsamide, a cyclic tetrapeptide from a marine *Nocardiopsis* sp., suppresses motility of colorectal cancer cells. *J. Nat. Prod.* **2020**, *83*, 3166–3172. [CrossRef]
15. Chen, W.M.; Sheu, F.S.; Sheu, S.Y. Novel L-amino acid oxidase with algicidal activity against toxic cyanobacterium *Microcystis aeruginosa* synthesized by a bacterium *Aquimarina* sp. *Enzym. Microb. Technol.* **2011**, *49*, 372–379. [CrossRef]
16. Helfrich, E.J.; Ueoka, R.; Dolev, A.; Rust, M.; Meoded, R.A.; Bhushan, A.; Califano, G.; Costa, R.; Gugger, M.; Steinbeck, C. Automated structure prediction of trans-acyltransferase polyketide synthase products. *Nat. Chem. Biol.* **2019**, *15*, 813–821. [CrossRef] [PubMed]
17. Vijayasarathy, S.; Prasad, P.; Fremlin, L.J.; Ratnayake, R.; Salim, A.A.; Khalil, Z.; Capon, R.J. C3 and 2D C3 Marfey's methods for amino acid analysis in natural products. *J. Nat. Prod.* **2016**, *79*, 421–427. [CrossRef]
18. Llinarés, J.; Elguero, J.; Faure, R.; Vincent, E.J. Carbon-13 NMR studies of nitrogen compounds. I—substituent effects of amino, acetamido, diacetamido, ammonium and trimethylammonium groups. *Org. Magn. Reson.* **1980**, *14*, 20–24. [CrossRef]
19. Luo, W.; Liu, Q.; Jiang, N.; Li, M.; Shi, L. Isorhamnetin inhibited migration and invasion via suppression of Akt/ERK-mediated epithelial-to-mesenchymal transition (EMT) in A549 human non-small-cell lung cancer cells. *Biosci. Rep.* **2019**, *39*, BSR20190159. [CrossRef]
20. Chen, K.-J.; Li, Q.; Wen, C.-M.; Duan, Z.-X.; Zhang, J.Y.; Xu, C.; Wang, J.-M. Bleomycin (BLM) induces epithelial-to-mesenchymal transition in cultured A549 cells via the TGF-β/Smad signaling pathway. *J. Cancer* **2016**, *7*, 1557. [CrossRef]
21. Agraval, H.; Yadav, U.C. MMP-2 and MMP-9 mediate cigarette smoke extract-induced epithelial-mesenchymal transition in airway epithelial cells via EGFR/Akt/GSK3β/β-catenin pathway: Amelioration by fisetin. *Chem.-Biol. Interact.* **2019**, *314*, 108846. [CrossRef]
22. Rhee, K.-H. Isolation and characterization of Streptomyces sp. KH-614 producing anti-VRE (vancomycin-resistant enterococci) antibiotics. *J. Gen. Appl. Microbiol.* **2002**, *48*, 321–327. [CrossRef] [PubMed]
23. Rhee, K.-H. Purification and identification of an antifungal agent from *Streptomyces* sp. KH-614 antagonistic to rice blast fungus, *Pyricularia oryzae*. *J. Microbiol. Biotechnol.* **2003**, *13*, 984–988.
24. Li, X.; Dobretsov, S.; Xu, Y.; Xiao, X.; Hung, O.S.; Qian, P.-Y. Antifouling diketopiperazines produced by a deep-sea bacterium, *Streptomyces fungicidicus*. *Biofouling* **2006**, *22*, 187–194. [CrossRef] [PubMed]

25. Gowrishankar, S.; Kamaladevi, A.; Ayyanar, K.S.; Balamurugan, K.; Pandian, S.K. Bacillus amyloliquefaciens-secreted cyclic dipeptide–cyclo (L-leucyl-L-prolyl) inhibits biofilm and virulence production in methicillin-resistant *Staphylococcus aureus*. *RSC Adv.* **2015**, *5*, 95788–95804. [CrossRef]
26. Abed, R.M.; Dobretsov, S.; Al-Fori, M.; Gunasekera, S.P.; Sudesh, K.; Paul, V.J. Quorum-sensing inhibitory compounds from extremophilic microorganisms isolated from a hypersaline cyanobacterial mat. *J. Ind. Microbiol. Biotechnol.* **2013**, *40*, 759–772. [CrossRef] [PubMed]
27. Gu, Q.; Fu, L.; Wang, Y.; Lin, J. Identification and characterization of extracellular cyclic dipeptides as quorum-sensing signal molecules from *Shewanella baltica*, the specific spoilage organism of *Pseudosciaena crocea* during 4 °C storage. *J. Agric. Food Chem.* **2013**, *61*, 11645–11652. [CrossRef]
28. Lin, C.-K.; Wang, Y.-T.; Hung, E.-M.; Yang, Y.-L.; Lee, J.-C.; Sheu, J.-H.; Liaw, C.-C. Butyrolactones and diketopiperazines from marine microbes: Inhibition effects on dengue virus type 2 replication. *Planta Med.* **2017**, *83*, 158–163. [CrossRef]
29. Jinendiran, S.; Teng, W.; Dahms, H.-U.; Liu, W.; Ponnusamy, V.K.; Chiu, C.C.-C.; Kumar, B.D.; Sivakumar, N. Induction of mitochondria-mediated apoptosis and suppression of tumor growth in zebrafish xenograft model by cyclic dipeptides identified from *Exiguobacterium acetylicum*. *Sci. Rep.* **2020**, *10*, 13721. [CrossRef]
30. Lind, H.; Sjögren, J.; Gohil, S.; Kenne, L.; Schnürer, J.; Broberg, A. Antifungal compounds from cultures of dairy propionibacteria type strains. *FEMS Microbiol. Lett.* **2007**, *271*, 310–315. [CrossRef]
31. Powers, J.C.; Baker, B.L.; Brown, J.; Chelm, B.K. Inhibition of chymotrypsin A. alpha. with N-acyl-and N-peptidyl-2-phenylethylamines. Subsite binding free energies. *J. Am. Chem. Soc.* **1974**, *96*, 238–243. [CrossRef] [PubMed]
32. Kim, J.H.; Bang, I.H.; Noh, Y.J.; Kim, D.K.; Bae, E.J.; Hwang, I.H. Metabolites Produced by the Oral Commensal Bacterium *Corynebacterium durum* Extend the Lifespan of *Caenorhabditis elegans* via SIR-2.1 Overexpression. *Int. J. Mol. Sci.* **2020**, *21*, 2212. [CrossRef] [PubMed]
33. Kunimoto, S.; Chin-Zhi, X.; Naganawa, H.; Hamada, M.; Masuda, T.; Tajeuchi, T.; Umezawa, H. Reversal of resistance by N-acetyltyramine or N-acetyl-2-phenylethylamine in doxorubicin-resistant leukemia P388 cells. *J. Antibiot.* **1987**, *40*, 1651–1652. [CrossRef] [PubMed]